Crystal supramolecular motifs. Ladders, layers and labyrinths of Ph₄P⁺ cations engaged in fourfold phenyl embraces

Marcia Scudder and Ian Dance [*]

School of Chemistry, University of New South Wales, Sydney 2052, Australia.
E-mail: I.Dance@unsw.edu.au

Tetraphenylphosphonium cations in crystals associate with attractive fourfold phenyl embraces (4PE), in which two phenyl rings from each cation engage in concerted edge-to-face and offset-face-to-face local interactions. The names of the orthogonal (O4PE) and parallel (P4PE) subclasses refer to the relationship between the relevant C–P–C planes in the two cations. One-dimensional ladder networks with O4PE along the sides and P4PE as rungs, and two-dimensional networks with O4PE in both directions, P4PE in both directions, or O4PE in one direction and P4PE in the other have been explored. The layers can be planar or corrugated. Crystalline $[Ph_4P^+][Cl_3Te(OCH_2CH_2O)]^-$ contains a zeolite-like network of cations involved in 4PE, with the anions in channels. Most of the crystals included in this survey contain mono-negative anions, ranging from Cl_3^- to metal complexes with chelate ligands, and include structurally non-molecular anions such as $[\{Cu_4I_5ReS_4\}^{2-}]_\infty$. The crystalline compound $[Ph_4P^+]_2[C_{60}]^-[I^-]_x$ contains a high symmetry two-dimensional network of cations in P4PE, which functions as an effective host lattice completely encapsulating the $[C_{60}]^-$, with phenyl$\cdots$fullerene interactions which are both face-to-face and edge-to-face.

Introduction

Our investigations of supramolecular motifs are based on the excellence of a molecular crystal as a supramolecular entity,[1,2] and the occurrence of crystallographic data for *ca.* 170,000 crystals (mainly of molecular compounds) in the Cambridge Structural Database.[3] One outcome has been the recognition of multiple phenyl embraces as significant supramolecular motifs for compounds containing Ph₄P⁺ cations and compounds with PPh₃ ligands.[4–6] While individual phenyl groups engage in edge-to-face (**ef**) and offset-face-to-face (**off**) attractive phenyl$\cdots$phenyl interactions, the multiple phenyl embraces are motifs in which these local attractions are concerted. The name embrace signifies the three attributes of (1) participation of two or more phenyl groups from each partner molecule, (2) geometrical concertedness, and (3) strong attraction.

The main categories of multiple phenyl embrace are the six-fold phenyl embrace or 6PE[†] containing six edge-to-face (**ef**) attractions involving three phenyl rings from each Ph₄P⁺, first identified by Muller,[7] and two types of fourfold phenyl embrace or 4PE.[†] In the orthogonal fourfold phenyl embrace (O4PE) the two C–P–C planes for the four phenyl rings are approximately orthogonal and engaged in four **ef** interactions, while in the parallel fourfold phenyl embrace (P4PE) these two C–P–C planes are approximately parallel and the motif comprises one **off** and two **ef** interactions.[6] The net attractive energy for the phenyl rings in the 6PE is calculated to be in the range 8–11 kcal mol⁻¹ (for a pair of complete Ph₄P⁺ cations the attractive energy is 5–8 kcal mol⁻¹):[‡] the energy of the 6PE is comparable with that of the stronger hydrogen bonds. The heteroaromatic rings of bipy ligands in [M(bipy)₃]ᶻ complexes can adopt similar sixfold aryl embraces,[8] and crystalline tris(anthracenyl)phosphine forms an inverted 6PE.[9]

We subsequently described the general occurrence of continuous chains of these embraces, as the zig-zag infinite chain of sixfold phenyl embraces (ZZI6PE, originally ZZISPE[†])[10] and the linear infinite chain of translational fourfold phenyl embraces (LIT4PE, originally LITQPE:[†] translational repetition of Ph₄P⁺ along a pseudo-twofold axis generates O4PE motifs).[6,10] Muller[11] had previously classified the columnar structures with fourfold crystal symmetry known in 1980. These one-dimensional extensions of the isolated embraces arise because each phenyl ring can function as both H "donor" and π "acceptor" in **ef** interactions. In the LIT4PE only two of the "edges" of the Ph₄P⁺ tetrahedron are involved in 4PE,[10] and therefore there are additional opportunities for multiple phenyl embraces. Similarly, in the ZZI6PE only two "faces" of the tetrahedron are used.[10] Both the LIT4PE and the ZZI6PE motifs could engage in additional embraces and form more highly connected supramolecular motifs, and it is these elaborations which are investigated in this and the following paper.

The Cambridge Structural Database (October, 1997) contains data for 1060 crystals containing Ph₄P⁺, and 944 of these contain at least one pair of cations with P$\cdots$P < 9 Å, signifying interpenetration of volumes and possible multiple phenyl embraces. Examination of this large collection of crystal structures reveals that more elaborate networks of multiple phenyl embraces occur. We classify these networks according to: (1) the number of connections at each Ph₄P⁺; (2) the embrace type; and (3) the dimensionality of the network. We have already described the group of compounds containing RPh₃P⁺ cations which crystallise with hexagonal arrays of 6PE (HA6PE[†]), which are further connected by other embraces.[12,13]

This paper focusses on one-, two- and three-dimensional networks constructed from 4PE, and the following paper[14] on networks based on 6PE.

---

† In our original papers the 6PE was named the sextuple phenyl embrace and abbreviated as SPE, and the 4PE was called the quadruple phenyl embrace, or QPE. Subsequent investigations of multiple phenyl embraces revealed more elaborate motifs involving larger numbers (eight and twelve) of phenyl rings, and so we have revised the abbreviations to include the number of phenyl rings involved.

‡ These intermolecular energies are calculated as the sum of the van der Waals and coulombic atom–atom components, dependent on empirical parameters which are under continuing refinement: more recent energy values may differ from earlier published values.

Table 1 Parameters used in calculations of interatomic energies: see eqns. (3), (4), (5)

Atom type	$A/Å^{12}$ kcal mol^{-1}	$B/Å^{12}$ kcal mol^{-1}	$d^a_i/Å$	$e^a_i/$kcal mol^{-1}	q_i
All C in phenyl ring	1116550.0	644.5	3.9	0.093	−0.10
All H in phenyl ring	23058.4	42.9	3.2	0.020	+0.15
P	6025894.0	2195.6	4.2	0.20	+0.40
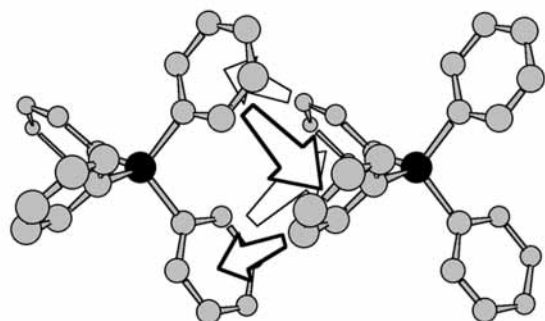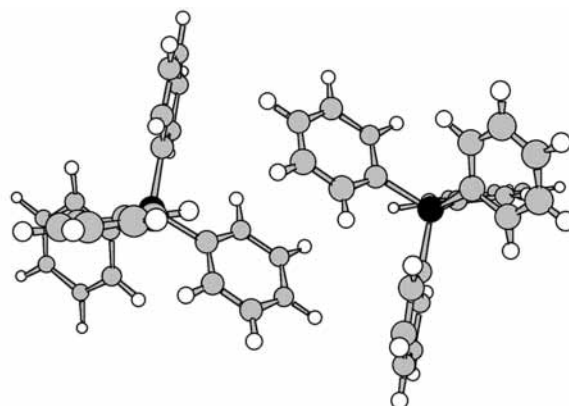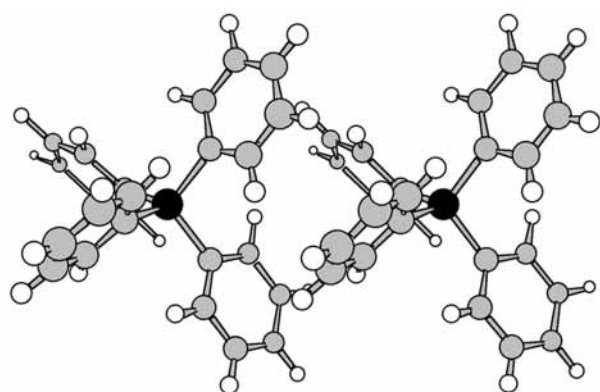
O4PE
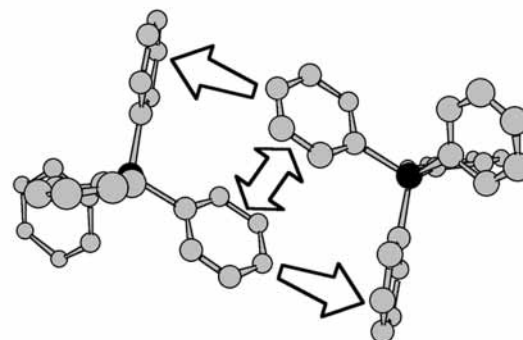
P4PE
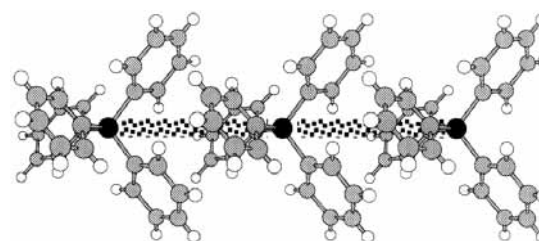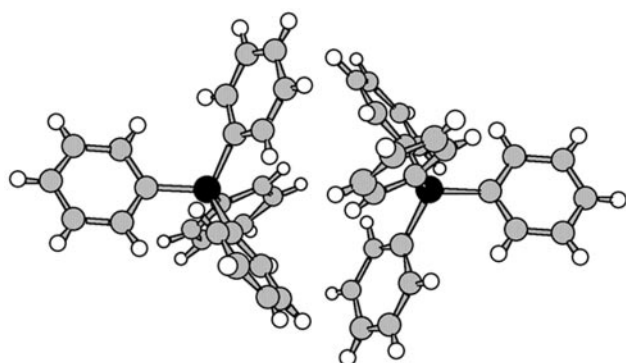
LIT4PE
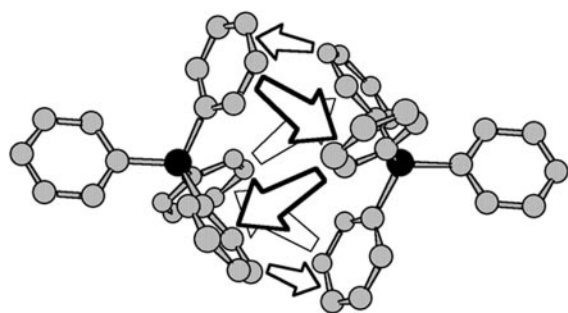
6PE

Methodology

Data were obtained from the October, 1997 release of the Cambridge Structural Database,[3,15] and analysed using the Cambridge Quest3D graphical software and the MSI programs [16] InsightII and Catalysis for construction, analysis and portrayal of crystal lattices.

Intermolecular energies E were calculated as the sum of interatomic energies,[17,18] using the Lennard-Jones 6-12 interatomic potential for attractive and repulsive van der Waals energies E^{vdW}_{ij} [eqn. (3)], and the coulombic components $E^{coulombic}_{ij}$ [eqn. (5)]. The atom partial charges q_i were obtained from a density functional (blyp) calculation of the electron density of Ph$_4$P$^+$ followed by optimisation of the charge array to best reproduce the electrostatic potential of Ph$_4$P$^+$. Because Ph$_4$P$^+$ has low polarity and no lone pairs, the coulombic energy need not incorporate atomic multipoles.[19] The van der Waals parameters have been refined to reproduce (together with the coulombic component) the best experimental and theoretical

Table 2 Crystal structures which contain isolated regular ladders of Ph_4P^+ cations. The interactions along the ladder edges are O4PE and the rungs are PQPE. In all crystals the ladders are parallel

| Refcode | Anion | Space group | P···P dimensions/Å | | Angle of rung to edges/° |
			Along ladder O4PE	Rungs, P4PE	
BITXUX	$[SnCl_3]^-$	$P\bar{1}$	7.42	8.20	78
BITYAE	$[SnBr_3]^-$	$P\bar{1}$	7.44	8.27	76
JETNUR	$[Cl_4Re(NSSN)]^-$	$P\bar{1}$	7.67	8.23	78
SAPDIW	$[Cu(SSNS)_2]^-$	$P\bar{1}$	7.08	8.99	79
TPCBPT	$[Cl_3Pt\{C(CH_2OH)\}_2]^-$	$P2_1/c$	7.47	8.56	79
VEJLAX	$[Cl_5W\{\eta^2\text{-}C(H)C(Ph)\}]^- \cdot CH_2Cl_2$	$P2_1/c$	7.51	8.00	76
WAKGUK	$[NCl_2Os(OCH_2CH_2O)]^-$	$P2_1/n$	8.17	8.61	88
YIMSUI	$[I_2(B_7CH_6)]^-$	$P\bar{1}$	7.84	8.50	83
ZUDPUJ	$[B_6H_6(CH_2CH_2)B_6H_6]^{2-}\cdot EtOH$	$P2_1/n$	7.53	8.53	69

information on the intermolecular energy of benzene. The parameters and charges used in eqns. (1) to (5) are presented in

$$E = \Sigma E_{ij} \quad (1)$$

$$E_{ij} = E^{vdW}_{ij} + E^{coulombic}_{ij} \quad (2)$$

$$E^{vdW}_{ij} = [(A_{ij} \times d_{ij})^{-12} - (B_{ij} \times d_{ij})^{-6}] = \\ e^a_{ij}[(d^a_{ij}/d_{ij})^{12} - 2(d^a_{ij}/d_{ij})^6] \quad (3)$$

$$A_{ij} = (A_i \times A_j)^{0.5}, \quad B_{ij} = (B_i \times B_j)^{0.5}, \\ d^a_{ij} = (d^a_i + d^a_j)/2, \quad e^a_{ij} = (e^a_i \times e^a_j)^{0.5} \quad (4)$$

$$E^{coulombic}_{ij} = q_i q_j/\varepsilon d_{ij} \quad (5)$$

Table 1: d_{ij} is the interatomic separation; A_{ij}, B_{ij} are the parameters used in the MSI program Discover;[16] e^a_{ij} and d^a_{ij} are respectively the energy depth and the interatomic distance for the attractive well of the vdW potential;[5] and the permittivity ε was set equal to d_{ij}.[5] In the Discussion the energies are considered per pair of $\{Ph_4\}$, and per Ph_4P^+ cation. The energies marked on the figures are per Ph_2 pair. Volumes were computed using a Connolly surface with a probe of zero radius, and van der Waals radii Cl 1.75 and Br 1.85 Å.

Results

One-dimensional arrays

When two strands of LIT4PE are located near each other so that embrace motifs occur between the strands, the result is a ladder. A regular ladder structure is illustrated in Fig. 1(a), for the compound $Ph_4P^+SnCl_3^-$ as it occurs in the crystals BITXUX (six letter identifiers for crystal structures are the reference codes of the Cambridge Structural Database). The rungs of the ladder are formed from P4PE. Fig. 1(b) shows more of the crystal lattice, and how the ladders are parallel and separated by the pyramidal $[SnCl_3]^-$ anions.

Table 2 lists other instances (with dimensions) of similar regular ladder structures comprised of O4PE along the edges and P4PE as rungs. The rungs of the ladder are approximately orthogonal to the edges, with the angle ranging from 69 to 88°. Note the variation in size and volume of the anions.

Another group of compounds has embracing cations in ladders comprised of triangular rather than quadrilateral segments. These compounds and the P···P dimensions of the
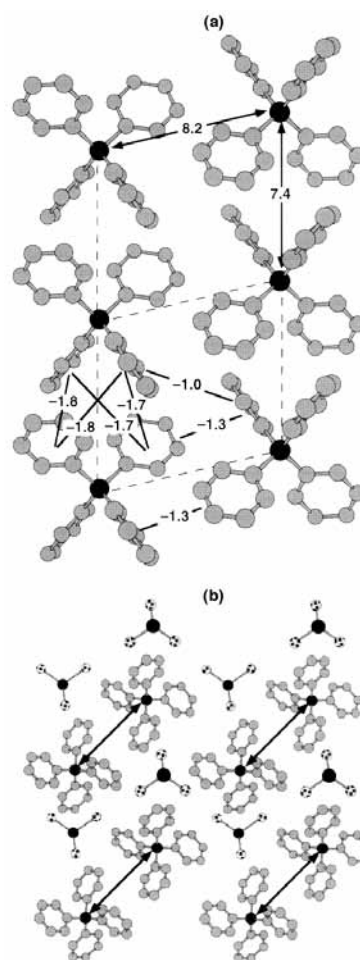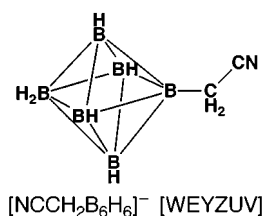
$[NCCH_2B_6H_6]^-$ [WEYZUV]

Fig. 1 Representations of the crystal packing in $Ph_4P^+SnCl_3^-$ [BITXUX]. (a) Two cells of the ladder of Ph_4P^+, with translationally repeated O4PE (7.4 Å) forming the ladder supports (vertical), and P4PE (8.2 Å) as the rungs: P black, C grey, H atoms omitted. P···P distances are marked with arrows, while the non-arrowed numbers are the interaction energies (kcal mol^{-1} per Ph_2) between phenyl rings. Ph···Ph energies smaller than 1.0 kcal mol^{-1} are not marked. There are centres of inversion on and between the rungs (space group $P\bar{1}$) with the c axis along the ladder. (b) View along the ladders (marked with arrows) showing the separation of the ladders by the pyramidal SnCl$_3^-$ anions: Sn black, Cl speckled.

ladders are listed in Table 3, and one example, WEYYUU, $Ph_4P^+[\mu\text{-}Br(NBS)_2]^-$ (NBS = N-bromosuccinimide), is illustrated in Fig. 2. The sides of the ladder are made up of O4PE (7.6 Å) while each of the zig-zag rungs involves an interaction between one ring from one cation and three from the other. The difference between this ladder and that shown in Fig. 1 can be easily visualised as being caused by a translation of one edge of the ladder relative to the other, by a distance of about half the

Table 3 Crystal structures with zig-zag ladder structures of the type shown in Fig. 2

| Refcode	Anion	Space group	Ladder dimensions $P\cdots P$ along, across/Å	Angles of rungs to edges/°	Relationship between ladders
FASWEB	$[V(SCH_2CH_2S)_2(OSiMe_3)]^-$	$P\bar{1}$	8.94, 8.75/8.04	62, 64, 54	Parallel
SELGOF	$[\{Cu_4I_5ReS_4\}^{2-}]_\infty\cdot CH_3CN$	$P2_12_12_1$	7.26, 8.88	66, 48, 66	Canted
TOPZIH	$[\{PbI_3\}^-]_\infty\cdot DMF$	$Pna2_1$	7.99, 8.65	63, 55, 63	Parallel
WEYYOO	$[\mu\text{-}Cl(NBS)_2]^-$	$P2_1/n$	7.64, 8.81	65, 51, 65	Parallel
WEYYUU	$[\mu\text{-}Br(NBS)_2]^-$	$P2_1/n$	7.62, 8.79	65, 51, 65	Parallel
WEZBAE	$[\mu\text{-}Cl(NIS)_2]^-\cdot CH_3CN$	$Pna2_1$	7.28, 8.98	66, 48, 66	Canted
WEZBEI	$[\mu\text{-}Br(NIS)_2]^-\cdot CH_3CN$	$Pna2_1$	7.25, 8.96	66, 48, 66	Canted

NIS = N-iodosuccinimide.
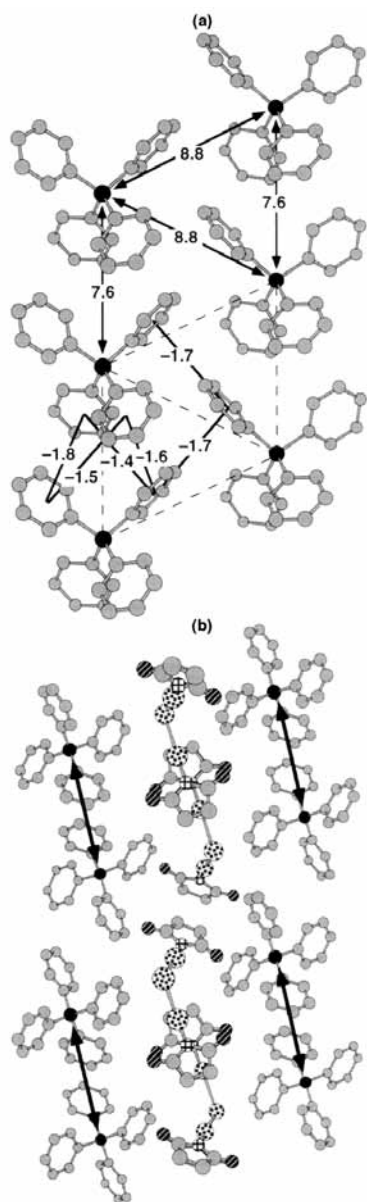
Fig. 2 Representations of the crystal packing in $Ph_4P^+[\mu\text{-}Br(NBS)_2]^-$ [WEYYUU]: P black, H atoms omitted for clarity. (a) Face view of the ladder: cell translation generates the O4PE along the ladder, while the rungs are generated by a 2_1 screw axis in space group $P2_1/n$. $P\cdots P$ distances are marked with arrows, while the non-arrowed numbers are the energies (kcal mol^{-1} per Ph_2) between phenyl rings. (b) View along the ladders (marked with arrows) showing how the ladders are separated by layers of $[\mu\text{-}Br(NBS)_2]^-$ anions. Br speckled, O striped, N cross-hatched.

O4PE length. Comparison of Figs. 1(b) and 2(b) shows that while there are differences within the ladders, both lattice types
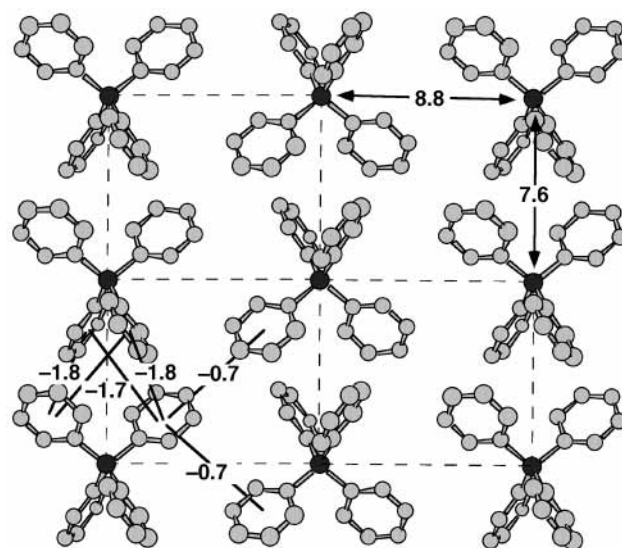

Fig. 3 The layer of Ph_4P^+ cations interacting attractively with O4PE (7.6 Å) and P4PE (8.8 Å) in crystalline $Ph_4P^+Br_3^-$ [BEPZEB]: $P\cdots P$ distances are marked with arrows. In space group $P2/c$ the net directions are b (7.6) and $c/2$ (8.8 Å): there are centres of inversion at the mid-points of the P4PEs. The P atoms (black) are coplanar. The Br_3^- anions are located between these layers. Non-arrowed numbers are the energies (kcal mol^{-1} per Ph_2) between phenyl rings.

have channels containing the anions between the ladders, and that the ladders are clearly separated by the anions, and confirm that the one-dimensional ladder entity is the primary supramolecular motif in these crystals. Just as ZZI6PE chains can be parallel or canted relative to each other,[10] these ladders also vary in their relative orientation, as shown in Table 3.

Two-dimensional arrays

Next we describe several classes of crystal packing which contain two-dimensional arrays of cations maintained by 4PE interactions. The first class of layer is propagated by O4PE in one direction and P4PE in the orthogonal dimension, with the P atoms exactly or nearly coplanar. This is illustrated in Fig. 3 for the compound $Ph_4P^+Br_3^-$ [BEPZEB]. This packing structure is the two-dimensional extension of the ladder shown in Fig. 1. The infinite sequences of O4PE in this layer are strong, as shown by the phenyl$\cdots$phenyl interaction energies marked on Fig. 3 for the embraces with a $P\cdots P$ separation of 7.6 Å (the interaction energy for the O4PE is -7.8 kcal mol^{-1} per $\{Ph_4\}_2$). The phenyl$\cdots$phenyl energies in the other dimension of the layer are weaker, and the interaction is a poor P4PE. Nevertheless, the integrity of this O4PE/P4PE layer is demonstrated by its general occurrence in a variety of compounds. Table 4 lists the relevant details of compounds with anions as varied as Br_3^-, Cl$^-$ (with $[Pr(OH_2)_6Cl_2]^+$ also in the lattice), and $[Cu(\eta^2\text{-}Cp)_2]^-$, which contain this layer motif of Ph_4P^+ cations. The anions are located between the layers.

Table 4 Crystal structures with two-dimensional nets of Ph_4P^+ cations, in which each cation is surrounded by four other cations and the net is propagated by O4PE motifs in one direction and by P4PE motifs in the other. All these nets have the P atoms exactly, or very nearly coplanar

Refcode	Anion and other components of the lattice	P$\cdots$P distance for the O4PE/Å	P$\cdots$P distance for the P4PE/Å
BEPZEB	$[Br_3]^-$	7.60	8.79
TPHOSI	$[BrIBr]^-$	7.67	8.88
CUPKAZ	$[(CO)_3Cr(\eta^5\text{-formylcp})]^-$	7.03	8.83
DALNAF01	$[Pr(OH_2)_6Cl_2]^+$, $2H_2O$, $2Cl^-$	6.71	8.21
HESJIY	$[CpLiCp]^-$	6.97	8.87
PPHTCQ	$[L_2]^-$	7.77	8.23
YIMSOC	$[I(B_7CH_7)]^-$	7.47	8.20, 8.93
YULLIA	$[Cr(CO)_5(NO_2)]^-$	6.95	8.94
YULLOG	$[W(CO)_5(NO_2)]^-$	7.05	8.98
YULYUZ	$[(BMe)_2B_4H_5]^-$	7.26	8.30
ZEZQOK	$[Cu(\eta^2\text{-Cp})_2]^-$	7.40	8.91

L = Tetracyanoquinodimethanide.

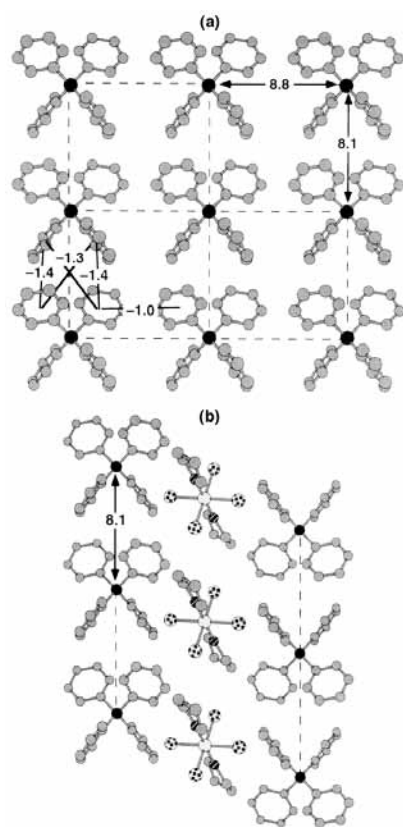**Fig. 4** Representations of the crystal structure of $Ph_4P^+[AsCl_4(THF)_2]^-$ [VUDTOD]. (a) The rectangular net of Ph_4P^+ cations involved in O4PE attractive interactions in both dimensions. The space group is $P2/c$: the 8.1 Å interaction is b, the 8.8 Å interaction is $a/2$. The calculated interaction energies per $\{Ph_4\}_2$ are -5.6 kcal mol^{-1} for the 8.1 Å O4PE, and -2.1 kcal mol^{-1} for the 8.8 Å O4PE: the total intralayer interaction energy per cation is -7.7 kcal mol^{-1} per $\{Ph_4\}$ [-2.2 kcal mol^{-1} per Ph_4P^+]. (b) Side view of two nets of cations sandwiching the $[AsCl_4(THF)_2]^-$ anions: As white, Cl speckled.

The second class of layer is a primitive rectangular net of repeating Ph_4P^+, which are oriented such that each Ph_4P^+ forms an O4PE with each of its four neighbours. The O4PEs which propagate the layer in one direction are shorter and more attractive than those in the other direction, as shown by the data in Fig. 4 for the compound $Ph_4P^+[AsCl_4(THF)_2]^-$ [VUDTOD]. We have identified only two other instances of this motif, listed in Table 5, but again we draw attention to the variety of anion type and shape which can be associated with this net.

The third type of two-dimensional net is propagated by P4PE embraces in both directions, as illustrated in Fig. 5 for the com-

pound $Ph_4P^+[SAs(S_7)]^-$ [KIYJIL]. Although the P4PE are longer than in isolated occurrences of this embrace, there are still strongly attractive $Ph\cdots Ph$ energies, as shown in Fig. 5(a). The slight distortions from a primitive square net of cations in this compound are due to the presence of the anion, which nestles in the cusps of the cation layer, as shown by the side view of the layers in Fig. 5(b).

Other instances of this P4PE/P4PE layer motif are listed in Table 6. We draw attention to the crystal packing in the three isostructural compounds which contain C_{60}^- as one of two anions, namely $[Ph_4P^+]_2[C_{60}]^-X^-$ (X = Cl, Br or I) [YEBDUE, YUXCAV, LAZPAD], illustrated in Fig. 6. Each layer of cations has a four-fold array of P4PE [Fig. 6(a)] in a high symmetry tetragonal ($I4/m$) lattice. These layers of cations are stacked according to mirror planes between them, such that the lattice contains tetragonal prismatic cavities surrounded by eight cations. The C_{60}^- and I^- ions occupy these cavities (although the I^- positions are incompletely occupied[20]). The I^- is surrounded by eight H atoms (the 4-positions of the phenyl rings), forming weak $C-H\cdots I$ hydrogen bonds [Fig. 6(a)]. The encapsulation of the C_{60}^- by the eight Ph_4P^+ cations is particularly significant and is described in more detail. Fig. 6(b) shows how the C_{60}^- nestles between four Ph_4P^+ cations engaged in four P4PE, and Fig. 6(c) showing the underside of this nest demonstrates how this square of four Ph_4P^+ in P4PE can almost completely cover the C_{60}^-. Most of the phenyl rings covering the C_{60}^- are in face(Ph)-to-face(C_{60}) geometry, as is common for C_{60} derivatives containing phenyl groups,[21–25] but four of the phenyl rings from each of the two layers approach the C_{60} in edge-to-face geometry: these four rings are evident in Fig. 6(b). Fig. 6(d) shows a side view of the C_{60} site, including cations from the cation layers above and below, and confirms that the C_{60} is almost totally covered by the eight cations.

In this crystal structure we see the two-dimensional array of Ph_4P^+ cations linked by P4PEs as indented with approximately hemispherical nests, able to hold a molecule such as C_{60} which engages in aryl$\cdots$aryl attractive interactions. Two such nests are able to enclose the fullerene. This role of the cation array is then comparable with that of host molecules of the calix-arene[26,27] and cyclotriveratrylene[28] classes. The host lattice formed by Ph_4P^+ cations using multiple phenyl embraces as the supramolecular factor is comparable with the hydrogen-bonded quinol networks which also include fullerenes.[29,30]

At this point we note that the rectangular layer motifs containing Ph_4P^+, in which each cation is surrounded by four other cations, can be propagated by O4PE in both dimensions, or P4PE in both dimensions, or by O4PE in one dimension and P4PE in the other. This is possible by rotations of the cations in the layers, as is evident by comparison of Figs. 3(a), 4(a) and 5(a).
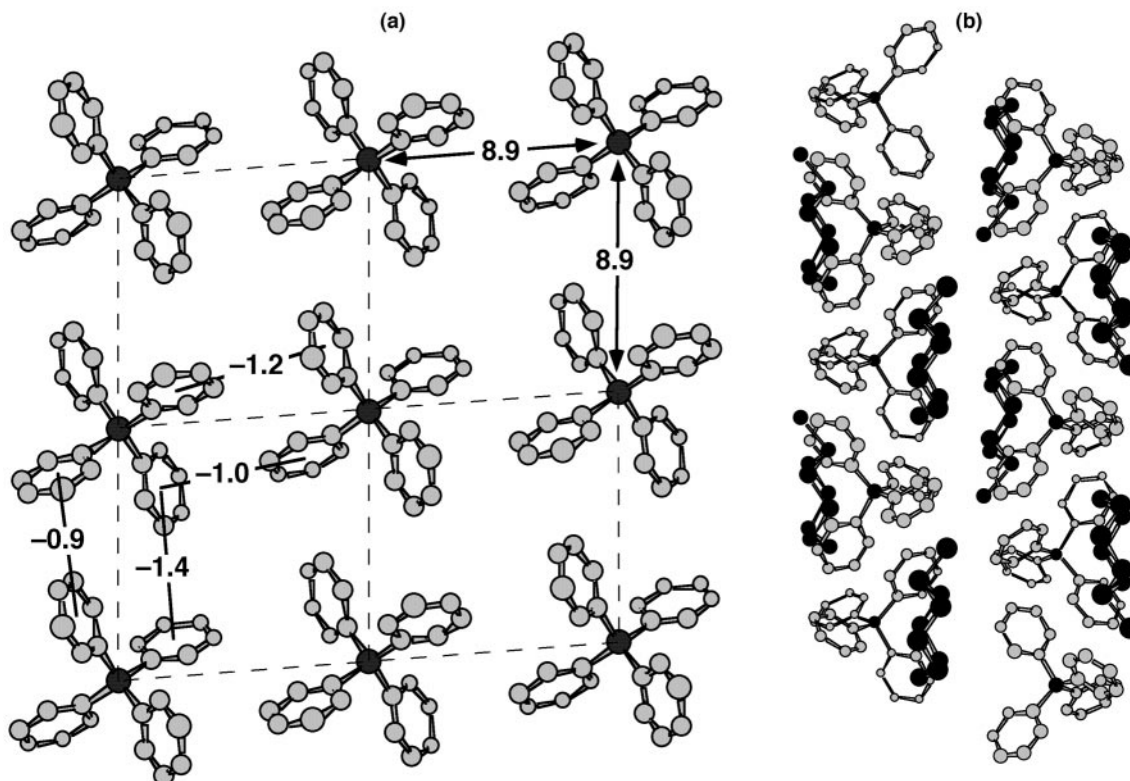
Fig. 5 Representations of the crystal packing in $Ph_4P^+[SAs(S_7)]^-$ [KIYJIL]. (a) The two-dimensional net of Ph_4P^+ cations involved in P4PE motifs in both dimensions. The space group is $Pna2_1$, and the net (generated by the n-glide operation) is along the two ab diagonals and is half the length of each. Ph$\cdots$Ph energies smaller than 0.9 kcal mol^{-1} are not marked. (b) Side view of two layers of cations, showing how the $[SAs(S_7)]^-$ anions (all atoms black) are positioned on the edges of the layers, not midway between them. The shortest S$\cdots$S distance between anions is 3.88 Å.

Table 5 Crystal structures with two-dimensional nets of Ph_4P^+ cations, in which each cation is surrounded by four other cations and the net is propagated by O4PE motifs in both directions

Refcode	Anion and other components of the lattice	Planarity of the net	P$\cdots$P distance for the shorter O4PE/Å	P$\cdots$P distance for the longer O4PE/Å
VUDTOD	$[Cl_4As(THF)_2]^-$	Flat	8.09	8.82
WEZVOM	$[L^1_2]$, Cl^-	Flat	7.46	7.97
YAPHUS	$[VL^2_2]^-\cdot H_2O$	Slightly pleated	7.81	8.55

L^1 = succinimide, $L^2 = {}^-O_2CCHMeN(O^-)CHMeCO_2{}^-$.

Table 6 Crystal structures with two-dimensional nets of Ph_4P^+ cations, in which each cation is surrounded by four other cations and the net is propagated by P4PE motifs in both directions

Refcode	Anion and other components of the lattice	Planarity of the net	P$\cdots$P distance for each embrace/Å
KIYJIL	$[SAs(S_7)]^-$	Flat	8.94
LAZPAD	$[C_{60}]^-$, I^-	Flat	8.90
YEBDUE	$[C_{60}]^-$, Cl^-	Flat	8.89
YUXCAV	$[C_{60}]^-$, Br^-	Flat	8.87

In the three types of two-dimensional four-connected nets already presented, the layers are exactly or almost planar, and there is only one type of embrace propagating the net in each dimension. There exists another class of two-dimensional four-connected nets which are corrugated and which have two different embraces alternating through the corrugations. The compounds which crystallise with this non-planar layer of four-connected cations are collected in Table 7, and one example, $Ph_4P^+[NCCH_2(B_6H_6)]^-$ [WEYZUV] is shown in Fig. 7.

$[NCCH_2B_6H_6]^-$ [WEYZUV]
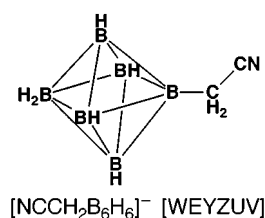
In addition to the corrugated layers just described, the four-connected net can be modified by part-translations of the linear sequences of principal motifs within the net in a way analogous to that described above for generation of the triangular ladder (Fig. 2) from the regular ladder (Fig. 1). This is best illustrated with the example of $[Ph_4P^+]_2[BrAg(\mu\text{-}Br)_2AgBr]^{2-}$ [GIDWEV] shown in Fig. 8. Now each cation is surrounded by five other cations, and has remarkably favourable attractive Ph$\cdots$Ph interactions with each of these cations. This could be called a five-connected net of embracing cations. Sections of the pleated layer have similarities to other motifs: the approximately rectangular section with P$\cdots$P distances of 7.5 and 7.9 Å is like the ladder in Fig. 1 while the triangular section is like the ladder in Fig. 2. Other compounds with this structure type are listed in Table 8.
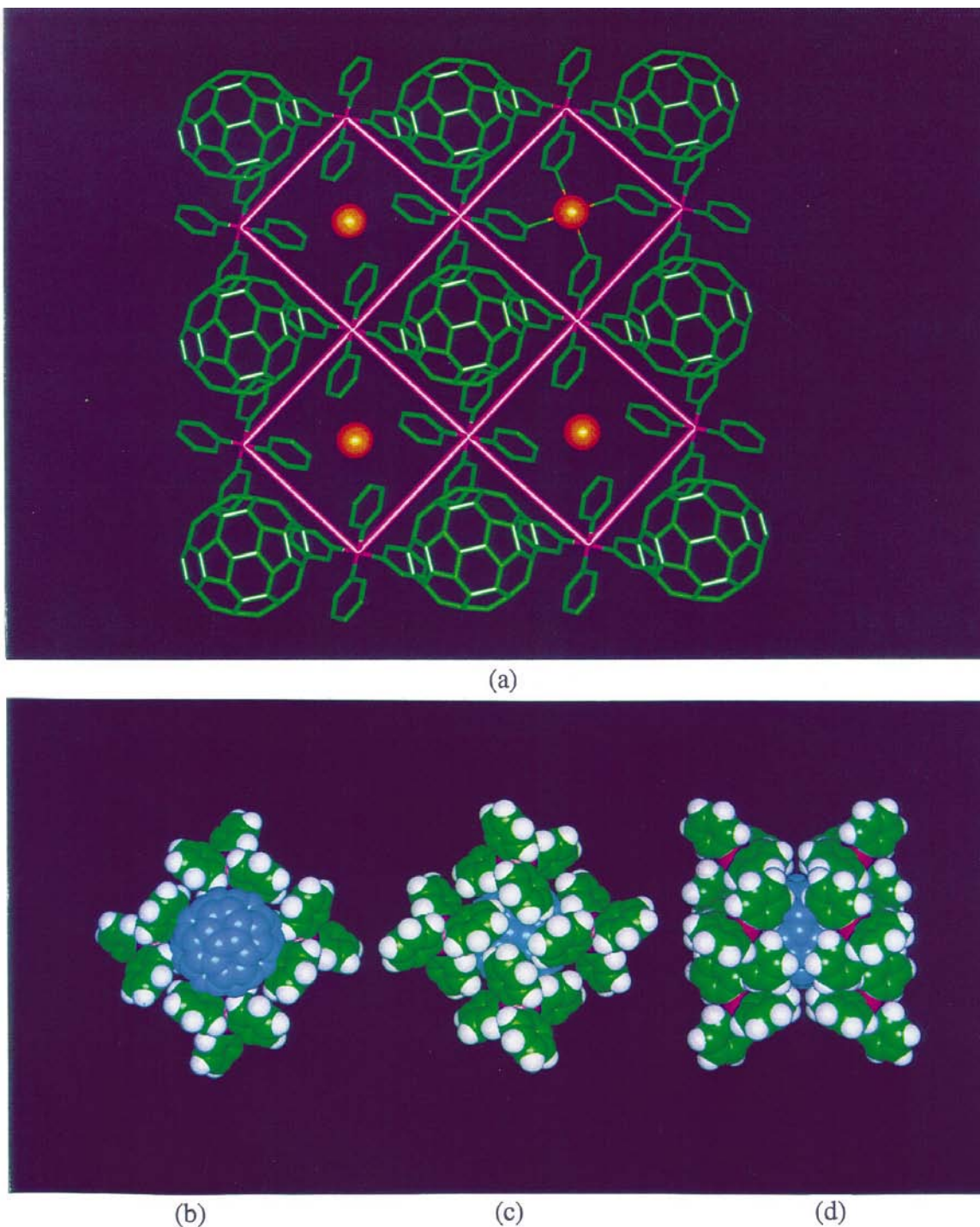
Fig. 6 Representations of the crystal packing in $[Ph_4P^+]_2[C_{60}]^-[I^-]_x$ [LAZPAD], space group $I4/m$. (a) View of the fourfold net of P4PE (purple rods) along ab diagonals of the cell, with the C_{60}^- anions (twofold disorder is not shown) located in cusps between four P4PE, and the I^- ions located on $4/m$ sites (with partial occupancy). The cations are at $\bar{4}$ sites, and the P4PE network is generated by the fourfold symmetry. The C_{60}^- and I^- ions are at the same z coordinate, and covered by the next net of cations above. The C–H$\cdots$I$^-$ weak hydrogen bonds (C$\cdots$I 3.67 and H$\cdots$I 2.82 Å) are marked in one quadrant. (b) Space-filling representation of the C_{60} anions nestled between the phenyl rings of four Ph_4P^+ cations engaged in four P4PE: note that there are face-to-face and edge-to-face interactions between Ph rings and C_{60}^-. (c) Underneath view of part (b), showing how the Ph_4P^+ cations completely enclose the C_{60}^-, and showing also the good edge-to-face and offset-face-to-face interactions of the P4PEs. (d) Side view of the two layers of embracing Ph_4P^+ cations almost completely enclosing the C_{60}^-: in this image the two layers of cations are drawn on the left and right rather than top and bottom. In parts (b), (c) and (d) the C_{60} has been coloured blue for contrast.

In addition to the linear chain, ladder or layer categories already described, there is a small number (less than 10 identified so far in the CSD) of structures with LIT4PE linked to form three-dimensional arrays of Ph_4P^+. One of them is $Ph_4P^+[Cl_3Te(OCH_2CH_2O)]^-$ [COETTE], which contains parallel LIT4PE chains which are linked in a hexagonal array to form a porous network akin to a zeolite, as shown in Fig. 9. The channels so formed contain double columns of anions. Each cation takes part in a total of five embraces. The O4PE (along a) has P$\cdots$P 7.5 Å and an interaction energy of -7.2 kcal

mol^{-1} per $\{Ph_4\}_2$. The additional interactions are a centrosymmetric P4PE with P$\cdots$P 9.0 Å and an interaction energy of -2.3 kcal mol^{-1} per $\{Ph_4\}_2$, and a second interaction with P$\cdots$P 8.2 Å and an energy of -5.9 kcal mol^{-1} per $\{Ph_4\}_2$.

Inter-Ph_4P^+ energies

The calculated inter-cation energies are the sum of the van der Waals and coulombic components, and are expressed in two ways: (a) as the energy due to the embracing phenyl rings, that is

Table 7 Crystal structures with two-dimensional nets of Ph_4P^+ cations, in which each cation is surrounded by four other cations and the net is pleated

Refcode	Anion and other components of the lattice	Planarity of the net	P···P distance (Å) and type for the principal propagating embrace	P···P distance (Å) and embrace type in the other dimension
FARXEB	$[Br_4W(\mu\text{-}S)(\mu\text{-}S_2)WBr_4]^{2-}$, CH_2Cl_2, H_2S	Pleated	7.53 O4PE	8.92
JAGMIN10	$[\{(\mu\text{-}Se_4)Ag\}^-]_\infty$	Pleated	7.08 O4PE	8.38, 8.82 both P4PE
WEYZUV	$[NCCH_2(B_6H_6)]^-$	Pleated	7.50 O4PE	8.34, 8.83 both P4PE
YAPHOM	$[VL_2]^-$	Pleated	7.92 O4PE	8.56
YEYXUV	$[In(SCH_2CH_2S)_2]^-$	Slightly pleated	7.36	8.96 O4PE
YIBLAW	$[I(B_6H_6)]^-$	Pleated	7.51 O4PE	8.23, 8.95 both P4PE
YUCSEU	$[Me(B_6H_6)]^-$	Pleated	7.41 O4PE	8.18, 8.73 both P4PE
ZEHTIP	Cl_3^-	Pleated	7.89 O4PE	8.14, 8.53 both P4PE

$L = ^-O_2CCH_2N(O^-)CH_2CO_2^-$.

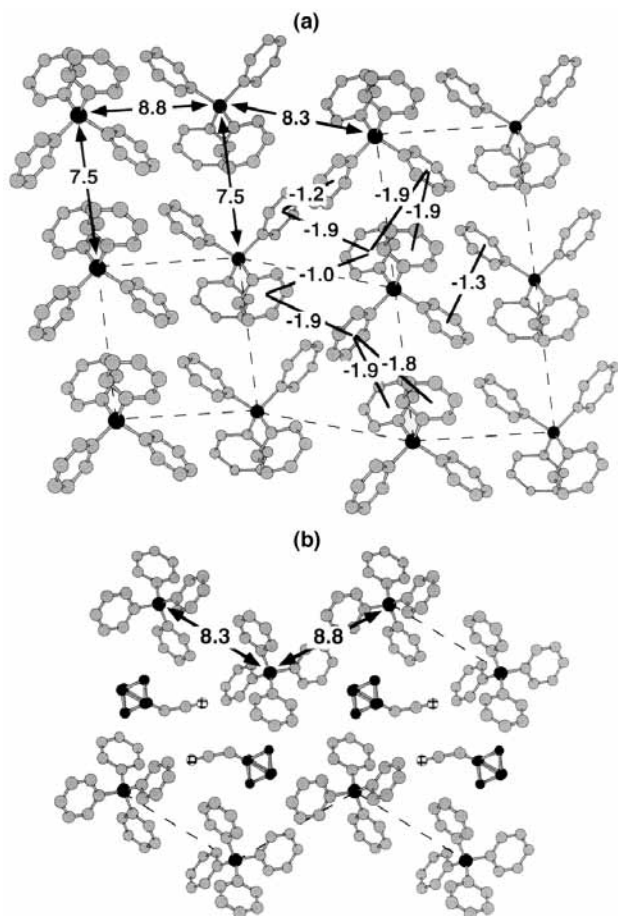**Fig. 7** Representations of the crystal structure of $Ph_4P^+[NCCH_2(B_6H_6)]^-$ [WEYZUV] which contains corrugated two-dimensional networks with O4PE and P4PE. (a) View towards the network. The 7.5 Å arrowed interaction is the O4PE (the cell a axis), and the 8.3 and 8.8 Å arrowed interactions are P4PEs. Ph···Ph energies smaller than 1.0 kcal mol^{-1} are not marked. The calculated energies between cations are -8.3 kcal mol^{-1} for the O4PE, -4.8 kcal mol^{-1} for the 8.3 Å pair, and -2.1 kcal mol^{-1} for the 8.8 Å interaction, all per $\{Ph_4\}_2$. Within the network the total interaction energy per cation is -12.6 kcal mol^{-1} [or -6.0 kcal mol^{-1} per Ph_4P^+]. (b) View parallel to the layers, showing their corrugation and the interleaving anions: B black.

Fig. 8 The two-dimensional network of Ph_4P^+ cations in $[Ph_4P^+]_2$-$[BrAg(\mu\text{-}Br)_2AgBr]^{2-}$ [GIDWEV]. There are centrosymmetric P4PEs with P···P 7.5 Å and calculated energy of -8.3 kcal mol^{-1}, O4PEs with P···P 7.9 Å (cell translation) and calculated energy of -4.8 kcal mol^{-1}, while the P···P 8.5 Å interactions occurring as a zig-zag generated by a 2_1 screw axis each involve a pair of phenyl rings with total energy -4.6 kcal mol^{-1}. Within the network the total interaction energy per cation is -13.8 kcal mol^{-1} [-6.6 kcal mol^{-1} per Ph_4P^+].

per pair of $\{Ph_4\}$, to focus on the reason for the embrace; (b) with inclusion of the additional contributions from the partially positive P atoms, and including all of the defined cation–cation interactions in the first sphere around Ph_4P^+ to give a total energy per sing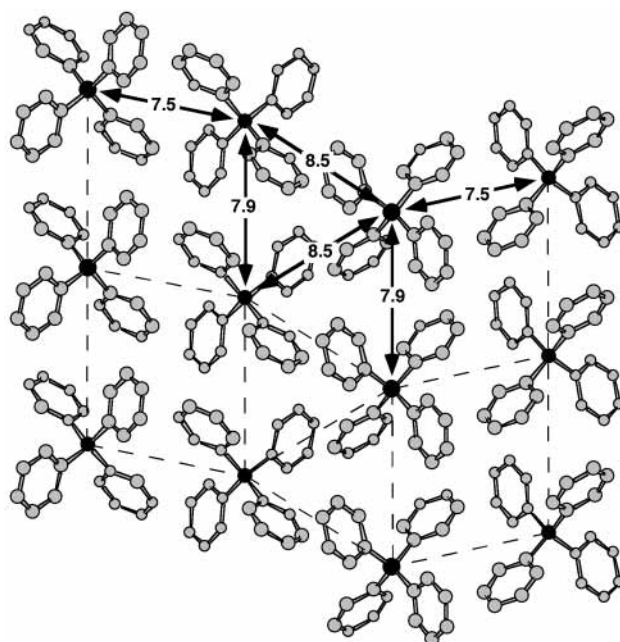le Ph_4P^+ cation. For the most common motifs, the sum of the additional contributions due to the P atoms is calculated to be $+3.3$ kcal mol^{-1} (per $\{Ph_4P^+\}_2$) for a 6PE, $+3.0$ kcal mol^{-1} (per $\{Ph_4P^+\}_2$) for an O4PE and $+2.8$ kcal mol^{-1} (per $\{Ph_4P^+\}_2$) for a P4PE. Table 9 summarises the calculated interaction energies for the various networks of embracing Ph_4P^+ cations.

In the ladder structures BITXUX and WEYYUU, the calculated interaction energies per $\{Ph_4\}$ for the components of the ladder are *ca.* -7 kcal mol^{-1} for the O4PE sides, and *ca.* -3 kcal mol^{-1} for the P4PE or other interactions as rungs. With inclusion of contributions from the P atoms, each cation in the ladder is attracted to neighbouring cations by -4.9 (BITXUX) or -3.3 (WEYYUU) kcal mol^{-1}. For the layered arrays of cations, the inter-cation energies within the layers vary according to the quality of the embraces: when assessed for the Ph rings alone the attractive energy per cation ranges from -4.8 to -13.8 kcal mol^{-1} in the best structure, $[Ph_4P^+]_2[BrAg(\mu\text{-}Br)_2$-

Table 8 Crystal structures with layers of Ph_4P^+ cations in which each cation is surrounded by five others, as in Fig. 8

| Refcode	Anion	P···P distances (Å) and motifs for principal chains in the layer	P···P distances (Å) for longer motifs
DEHKAC	$[ICu(\mu\text{-}I)_2CuI]^{2-}$	7.82 O4PE	7.69 P4PE, 8.57
GIDWEV	$[BrAg(\mu\text{-}Br)_2AgBr]^{2-}$	7.91 O4PE	7.48 P4PE, 8.46
KEWFEX	$[\{(\mu\text{-}I)(\mu_3\text{-}I)_2(\mu_4\text{-}I)Ag_3\}^-]_\infty$	8.50 O4PE	7.78, 8.85, 8.87 all P4PE
SEHFUG	$[F_2Cl_2Re(NSSN)]^-$	7.13 O4PE	8.90 P4PE, 8.95
SIHRAC	$[(CO)_4MoL]^-$	7.48 O4PE	8.56 P4PE, 8.94
TUJYEC	$[SeCl_4]^{2-}, (CH_3CN)_2$	7.26 O4PE	8.26 P4PE, 8.92
WEZVUS	$[\mu\text{-}Cl(NClS)_2]^-$	7.53 O4PE	8.73, 8.98 P4PE

L = 2,2'-bipyridine-5-sulfonate.
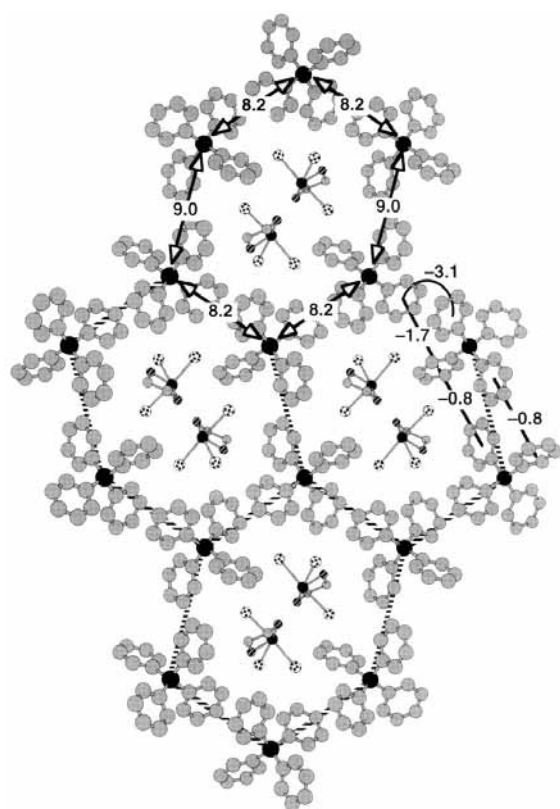
Fig. 9 The three-dimensional network of Ph_4P^+ cations in $[Ph_4P^+]$-$[Cl_3Te(OCH_2CH_2O)]^-$ [COETTE] viewed along the LIT4PE chains, with the pseudo-hexagonal array of these chains outlined. The independent P···P distances and prominent Ph···Ph energies are marked. In the O4PE which are perpendicular to the plane of this figure, the individual Ph···Ph energies for the four **ef** interactions are −1.4, −1.4, −1.9 and −1.9 kcal mol^{-1}. The anions are located in pairs within the channels in the cation network: Te black, Cl speckled.

$AgBr]^{2-}$ [GIDWEV] (Fig. 8) which has corrugations and displacements in the layers. For this structure the full calculated energy for each cation with its surrounding cations is −6.6 kcal mol^{-1}. Only the poorest of the layered motifs, $Ph_4P^+[SAs(S_7)]^-$ [KIYJIL], has a small (0.7 kcal mol^{-1}) net repulsion between cations. The three-dimensional network of Ph_4P^+ using 4PE, [COETTE] (Fig. 9), has a total interaction energy per cation of −6.7 kcal mol^{-1} per Ph_4P^+.

Discussion

We have shown instances of Ph_4P^+ embracing mainly through 4PE in the six different network types shown in Fig. 10, and also a three-dimensional network. A total of 43 different crystal structures and 50 different compounds are included in this classification. The LIT4PE network, Fig. 10(a), was described previously[10] (and there are now some 70 structures in the 1997 CSD which adopt this motif) while the others are new. There
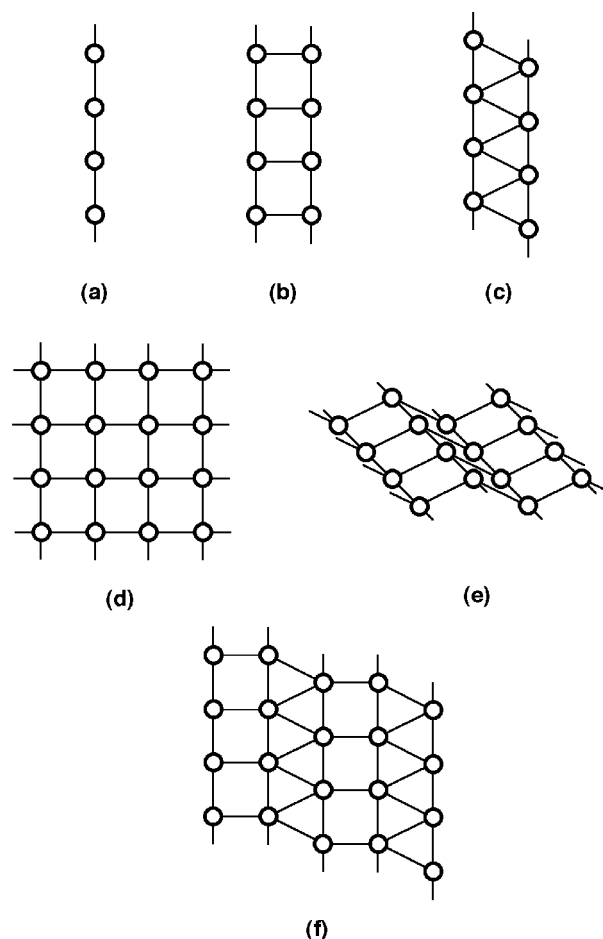
Fig. 10 Networks of Ph_4P^+ cations (symbolised as circles) in crystals, representing the one- and two-dimensional concerted supramolecular motifs comprised of fourfold phenyl embraces. (a) is the same as the LIT4PE. The connecting lines represent well-defined local 4PE (or in some instances, embraces involving three phenyl rings) in some crystals. In many crystals the concerted supramolecular motif is considered to be the complete network, which is more significant than the local 4PE.

are two types of ladder, where the sides are constructed from O4PE [Fig. 10(b) and Fig. 10(c)]. The rectangular array of Fig. 10(d) has been demonstrated with orthogonal 4PE in both directions, parallel 4PE in both directions, and with O4PE in one direction and P4PE in the other: these variations arise by rotation of the Ph_4P^+ cations about real or pseudo-two-fold axes in or perpendicular to the layer plane. In general the O4PEs in these nets are tighter and more attractive than the P4PEs. The O4PE usually results from unit cell translation (and hence very many of the compounds described here have one cell dimension of about 7.5 Å), while the P4PE often surrounds a centre of symmetry. The relative conformations of the two rings on each cation which form the P4PE dictate its quality. The P4PE has two components, the **off** interaction and the two **ef**

Table 9 Summary of the energy components (kcal mol^{-1}) for interacting cations in the networks described

Refcode	O4PE[a]	P4PE[a]	Other interactions[a]	Total For Ph rings[b]	For Ph$_4$P$^{+\,c}$
Ladder					
BITXUX	−7.8	−3.3		−10.0	−4.9
WEYYUU	−6.8		−2.6	−9.4	−3.3
Layer					
BEPZEB	−7.8	−0.5		−8.8	−2.4
VUDTOD	−5.6, −2.1			−7.7	−2.2
KIYJIL		−2.7, −2.1		−4.8	+0.7
WEYZUV	−8.3	−4.8, −2.1		−12.6	−6.0
GIDWEV	−4.8	−8.3	−4.6	−13.8	−6.6
Labyrinth					
COETTE	−7.2	−2.3	−5.9	−15.1	−6.7

[a] Energy per {Ph$_4$}$_2$ due to the embracing phenyl rings. [b] Energy, per cation, summed over the Ph$\cdots$Ph interactions for Ph$_4$P$^+$ ions in the first sphere around Ph$_4$P$^+$. [c] Energy, per Ph$_4$P$^+$, summed over the identified Ph$_4$P$^+\cdots$Ph$_4$P$^+$ interactions to the first sphere around Ph$_4$P$^+$.

interactions, but the energy derived from the **off** interaction is the one which dominates the total energy of the interaction, and as a result there is wide variability in the energy associated with the P4PE.

Ladders can be parallel, or canted: parallel ladders can be coplanar, or not. When they are coplanar, the obvious comparison is of the ladder (*e.g.* BITXUX, Table 2, Fig. 1) with a layer (*e.g.* BEPZEB, Table 4, Fig. 3), created simply by moving the ladder edges closer together. When the ladders are not coplanar, they can be envisaged as creating puckered layers when brought closer together. In both WEYYOO and WEYYUU (Table 3) the ladders are slightly non-coplanar, and when brought closer together form the slightly puckered layer of the isomorphous WEZVUS (Table 8). In JETNUR (not pictured) the ladders are distinctly non-coplanar.

In the crystal packing arrangements classified in this paper there are segregated regions of cations and anions. This distinction from the conventional desegregated array of ions of opposite charge emphasises again[10,13] that the packing in crystals containing arylated cations, such as Ph$_4$P$^+$, is frequently dominated by *attractive interactions between cations*. The common occurrence of the identified cation–cation motifs in crystals with different anions indicates that these cation-based supramolecular features could be more significant than cation–anion interactions. The anions in the compounds surveyed in this paper generally do not have arylated surfaces (C$_{60}^-$ is the exception) and are not able to participate in phenyl embraces. In a subsequent paper we will describe the crystal supramolecularity which occurs when the anion is also able to engage in multiple phenyl embraces, as for example in Ph$_4$P$^+$Ph$_4$B$^-$ and related compounds.[31]

The size and shape of the anion are clearly factors in determining the crystal packing in a particular structure. The anions in the compounds included in this analysis are generally approximately the same size as the cation, although in some cases are smaller, for example [SnCl$_3$]$^-$ [BITXUX] and Br$_3^-$ [BEPZEB]. Crystals of Ph$_4$P$^+$ with the comparable anions Br$_3^-$, BrIBr$^-$ and Cl$_3^-$ are included in this survey. The first two are isostructural and form planar layer structures created by O4PE in one direction and P4PE in the other, but Ph$_4$P$^+$Cl$_3^-$ contains a highly puckered layer. While the shape of the anions is the same, there is a significant difference in their volumes: Br$_3^-$ 73 Å^3, Cl$_3^-$ 60 Å^3.

Only those crystals in which the anion is slightly larger than the cation form the P4PE/P4PE layer, namely [SAs(S$_7$)]$^-$ [KIYJIL] and the three C$_{60}^-$X$^-$ compounds. The larger anions appear to distend and weaken the cation array, as is evident by comparison of the energies for KIYJIL with the others in Table

9. In the case of the three C$_{60}^-$X$^-$ compounds there are compensating attractions between the cations and C$_{60}^-$, and between the cations and X$^-$. Why then does KIYJIL have a structure similar to the C$_{60}^-$ compounds? The shape of the anion is not dissimilar to one half of a C$_{60}$ molecule, and so it fits neatly into the same nest. There are attractive S$\cdots$phenyl interactions which add stability to this arrangement [Fig. 5(b)].

In some of the networks described in this paper there are local phenyl$\cdots$phenyl attractions involving more than two cations [see Figs. 1(a), 3, 7(a)], and therefore the networks are more than the sums of the standard phenyl embraces for cation pairs. We regard these larger networks as the concerted supramolecular motifs demonstrated by these crystals. As for our previous classifications of the ZZI6PE and the LIT4PE as one-dimensional supramolecular motifs based on multiple phenyl embraces, we consider that the networks illustrated in Fig. 10 provide a valuable conceptual foundation of concerted supramolecular motifs for crystal engineering using Ph$_4$P$^+$ cations. In support of this contention we note that the crystal structures described in this paper are free of crystallographic disorder of the cations, indicating the significance of these extended multiple phenyl embraces.

In the following paper[14] we describe further two- and three-dimensional networks of Ph$_4$P$^+$ cations in crystals, where the 6PE is the dominant pairwise motif.

References

1 J. D. Dunitz, *Pure Appl. Chem.*, 1991, **63**, 177.
2 G. R. Desiraju, *The Crystal as a Supramolecular Entity*, *Perspectives in Supramolecular Chemistry*, ed. J. M. Lehn, John Wiley, Chichester, 1996.
3 F. H. Allen and O. Kennard, *Chem. Des. Automat. News*, 1993, **8**, 131.
4 I. G. Dance and M. L. Scudder, *J. Chem. Soc., Chem. Commun.*, 1995, 1039.
5 I. G. Dance, in *The Crystal as a Supramolecular Entity*, ed. G. R. Desiraju, John Wiley, New York, 1996, pp. 137–233.
6 I. Dance and M. Scudder, *Chem. Eur. J.*, 1996, **2**, 481.
7 U. Muller, P. Klingelhofer, J. Eicher and R. Bohrer, *Z. Kristallogr.*, 1984, **168**, 121.
8 I. Dance and M. Scudder, *J. Chem. Soc., Dalton Trans.*, 1998, 1341.
9 I. Dance and M. Scudder, *Polyhedron*, 1997, **16**, 3545.
10 I. Dance and M. Scudder, *J. Chem. Soc., Dalton Trans.*, 1996, 3755.

11 U. Muller, *Acta Crystallogr.*, *Sect. B*, 1980, **36**, 1075.
12 C. Hasselgren, P. A. W. Dean, M. L. Scudder, D. C. Craig and I. G. Dance, *J. Chem. Soc.*, *Dalton Trans.*, 1997, 2019.
13 M. Scudder and I. Dance, *J. Chem. Soc.*, *Dalton Trans.*, 1998, 329.
14 M. Scudder and I. Dance, following paper.
15 F. H. Allen, J. E. Davies, J. J. Galloy, O. Johnson, O. Kennard, C. F. Macrae and D. G. Watson, *Chem. Inf. Comput. Sci.*, 1991, **31**, 204.
16 MSI, *http://www.msi.com*, 1998.
17 A. J. Pertsin and A. I. Kitaigorodsky, *The atom-atom potential method. Applications to organic molecular solids*, Springer Series in Chemical Physics, Springer-Verlag, Berlin, 1987.
18 A. Gavezzotti, *Theoretical Aspects and Computer Modelling of the Molecular Solid State*, *Molecular Solid State Series*, John Wiley, Chichester, 1997.
19 D. S. Coombes, S. L. Price, D. J. Willock and M. Leslie, *J. Phys. Chem.*, 1996, **100**, 7352.
20 A. Penicaud, A. Perez-Benitez, R. Gleason, E. Munoz and R. Escudero, *J. Am. Chem. Soc.*, 1993, **115**, 10392.
21 A. L. Balch, V. J. Catalano and J. W. Lee, *Inorg. Chem.*, 1991, **30**, 3980.
22 A. L. Balch, V. J. Catalano, J. W. Lee, M. M. Olmstead and S. R. Parkin, *J. Am. Chem. Soc.*, 1991, **113**, 8953.
23 A. L. Balch, V. J. Catalano, J. W. Lee and M. M. Olmstead, *J. Am. Chem. Soc.*, 1992, **114**, 5455.
24 A. L. Balch, J. W. Lee and M. M. Olmstead, *Angew. Chem.*, *Int. Ed. Engl.*, 1992, **31**, 1356.
25 A. L. Balch, J. W. Lee, B. C. Noll and M. M. Olmstead, *J. Chem. Soc.*, *Chem. Commun.*, 1993, 56.
26 J. L. Atwood, G. A. Koutsantonis and C. L. Raston, *Nature* (*London*), 1994, **368**, 229.
27 C. L. Raston, J. L. Atwood, P. J. Nichols and I. B. N. Sudria, *Chem. Commun.*, 1996, 2615.
28 J. L. Atwood, M. J. Barnes, M. G. Gardiner and C. L. Raston, *Chem. Commun.*, 1996, 1449.
29 O. Ermer and C. Röbke, *J. Am. Chem. Soc.*, 1993, **115**, 10077.
30 O. Ermer, *Helv. Chim. Acta*, 1991, **74**, 1339.
31 B. F. Ali, D. C. Craig, I. G. Dance, A. D. Rae and M. L. Scudder, unpublished work.